

# A Biophysical Analysis of Stem and Root Diameter Variations in Woody Plants

Michel Génard\*, Svetlana Fishman, Gilles Vercambre, Jean-Gérard Huguet, Claude Bussi, Jacques Besset, and Robert Habib

Unité de Recherche en Ecophysiologie et Horticulture, Institut National de la Recherche Agronomique, Domaine Saint-Paul, Site Agroparc, 84914 Avignon cedex 9, France (M.G., G.V., J.-G.H., R.H.); Department of Statistics and Operations Research, Agricultural Research Organization, The Volcani Center, Bet Dagan 50250, Israel (S.F.); and Unité Expérimentale de Recherche Intégrée, Institut National de la Recherche Agronomique, Domaine de Gotheron, 26320 Saint-Marcel-les-Valences, France (C.B., J.B.)

A comprehensive model of stem and root diameter variation was developed. The stem (or root) was represented using two coaxial cylinders corresponding with the mature xylem and the extensible tissues. The extensible tissues were assumed to behave as a single cell separated from the mature xylem by a virtual membrane. The mature xylem and the extensible tissues are able to dilate with temperature and grow. Moreover, the extensible tissues are able to shrink and swell according to water flow intensity. The model is mainly based on the calculation of water volume flows in the "single cell" that are described using the principles of irreversible thermodynamics. The elastic response to storage volume and plastic extension accompanying growth are described. The model simulates diameter variation due to temperature, solute accumulation, and xylem, water potential. The model was applied to the peach (*Prunus persica*) stem and to the plum (*Prunus domestica* × *Prunus spinosa*) root. The simulation outputs corresponded well with the diameter variation observed. The model predicts that variations of turgor pressure and osmotic potential are smaller than the variations of xylem water potential. It also demonstrates correlations between the xylem water potential, the turgor pressure, the elastic modulus, and the osmotic potential. The relationship between the diameter and the xylem water potential exhibits a substantial hysteresis, as observed in field data. A sensitivity analysis using the model parameters showed that growth and shrinkage were highly sensitive to the initial values of the turgor pressure and to the reflection coefficient of solutes. Shrinkage and growth were sensitive to elastic modulus and wall-yielding threshold pressure, respectively. The model was not sensitive to changes in temperature.

Variations in size of organs result from changes in hydration, temperature, and growth. Size variation, caused by recurrent shrinking and swelling that are a function of the changing levels of hydration, may greatly exceed those resulting from daily growth of tissues or direct temperature variations (Kozłowski, 1972). Shrinking and swelling take place in extensible tissues found mainly in a narrow ring outside the dead xylem vessels in woody stems (Molz and Klepper, 1973; Zimmerman and Milburn, 1982; Brough et al., 1986), given that xylem tissues are almost totally rigid. Daily shrinkage in plant stem is related to variation in water potential (Klepper et al., 1971; Garnier and Berger, 1986), indicating that the higher the water stress, the more the water compartment of the plant is depleted during the day. However, the relationship between stem water potential and stem diameter changes throughout the day, showing a marked hysteresis. For a given water potential, a greater diameter is generally observed in the morning than in the afternoon (Klepper et al., 1971; Garnier and Berger, 1986).

Molz and Klepper (1972) presented a theory for cotton stem shrinking and swelling. This theory as-

sumed that water flows are driven by water potential differences between the adjacent cell layers of extensible tissues. From a mathematical point of view, this leads to the use of a diffusion type of kinetics for the propagation of water content variation in isotropic and homogeneous tissues. Parlange et al. (1975) adapted Molz and Klepper's model, considering that the diffusion coefficient increases as the medium becomes wetter, and obtained good results for tree stems. These models do not take the water storage capacity in cells into consideration. This storage capacity was included in the theoretical development of Molz and Ikenberry (1974) for water transport through cells and cell walls. Steudle and coworkers (for review, see Steudle and Peterson, 1998) more recently proposed an extended theory of water transport in root tissues: The water is transported by bulk flow through a composite membrane, which was considered to be built from "membrane-like elements arranged both in series and in parallel."

On a long-term basis, diameter variation also depends on growth. Water influx into the cells leads to irreversible changes in volume if it is accompanied by cell wall extension. The most widely used model of cell expansion was developed by Lockhart (1965). According to this model, cell expansion can be described using cell turgor pressure, cell wall extensi-

\* Corresponding author; e-mail Michel.Genard@avignon.inra.fr; fax 33-432-72-24-32.

bility ( $\phi$ ), and turgor pressure at which wall yielding (Y) occurs. Lockhart's equation (1965) has been used in a number of recent studies (Arkebauer et al., 1995; Fishman and Génard, 1998).

The aim of this study was to develop a mechanistic model for stem and root diameter variation, based on a biophysical representation of water transport by bulk flow while taking into account the water storage capacity of extensible living tissues. Diameter variations were assumed to be the result of changes in water storage and temperature as well as growth, which was stimulated by turgor pressure according to Lockhart's equation (1965). The model was applied to the simulation of stem and root diameter variation under various plant water conditions. The results of the simulations were compared with experimental results obtained on peach (*Prunus persica*) stems and plum (*Prunus domestica*  $\times$  *Prunus spinosa*) roots. The variations in osmotic and water potentials, turgor pressure, and elastic modulus of the storage compartment were analyzed. The sensitivity of diameter variation to the model parameters was studied and the effect of some of these parameters on the hysteresis between water potential and diameter changes was discussed.

## SIMULATION MODEL

The framework developed here made it possible to build a comprehensive model of stem and root diameter variation in response to xylem water potential and temperature. The model is based on major biophysical processes such as water fluxes and thermal, elastic, and plastic variations.

The model simulates the stem (root) diameter variation according to temperature, solute accumulation, and water input or output in response to xylem water potential. The stem (root) is modelled using two coaxial cylinders separated by a membrane (Fig. 1). It is assumed that the mature xylem forms a continuous rigid cylinder bound by an outer ring composed of the different extensible tissue (phloem, immature xylem, cortex, and cork cambia). The external cylinder is considered as the storage compartment, leading to shrinking and swelling with the horizontal water flux from or to the xylem. The external cylinder behaves as a single cell, separated from the xylem by a virtual membrane. The virtual membrane is composed of membranes and cell walls of several cell layers leading to cell-to-cell and apoplastic water flow between the "single cell" and the xylem. This virtual membrane is similar to the composite membrane defined by Steudle et al. (1993) to model solution transport to the root xylem.

A "single cell" approach to storage compartments made it possible to simplify the theoretical analysis and to clarify the relationships between basic mechanisms and an internal system of feedback control.

All the tissues are able to dilate with temperature and grow. The model is mainly based on the calcula-

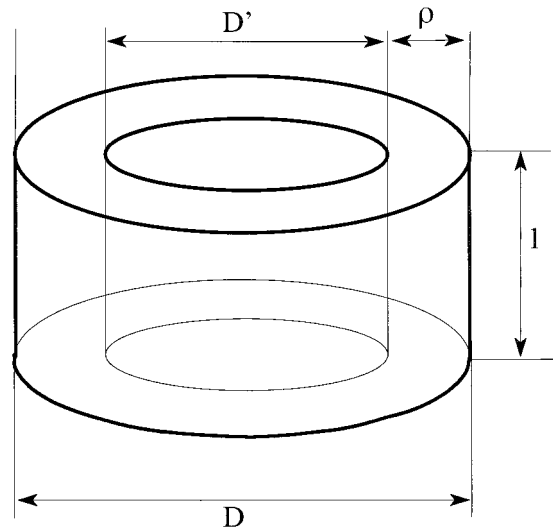


**Figure 1.** Geometry of the system. The stem (root) of diameter  $D$  is modeled by a system made of two coaxial cylinders of length  $l$  separated by a membrane. The mature xylem is represented by the inner cylinder of diameter  $D'$ . The extensible tissues are represented by the external cylindrical layer of thickness  $\rho$ .

tion of water volume flows, which are described using the principles of irreversible thermodynamics (Katchalsky and Curran, 1965). The elastic response to storage volume and plastic extension accompanying growth are described. The time frame that the model used to predict the diameter variation is between a day and two weeks. A list of the model variables and parameters is presented in Tables I and II.

## Geometry

The stem (root) diameter,  $D$  (m), equals the diameter of the outer cylinder in Figure 1. The mature xylem with a diameter  $D'$  (m) is represented by the inner cylinder. The thickness of the storage compartment is equal to:

$$\rho = (D - D')/2 \quad (1)$$

The volume of the storage compartment ( $V$  in  $\text{m}^3$ ) depends on its thickness:

$$V = \pi \rho D' l (1 + \rho/D') \quad (2)$$

where  $l$  is a constant equal to the length unit of the axis. A first approximation is carried out to simplify further analyses, where the thickness  $\rho$  is assumed to be much lower than the diameter  $D'$ . This makes it possible to transform equation 2 into:

$$V \cong \pi \rho D' l \quad (3)$$

Using an empirical relationship between  $\rho$  and  $D$  (see Eq. 13), it can be shown that the error resulting from this approximation is always less than 10% and it is less than 5% for diameters greater than 5 cm.

**Table 1.** *Model variables*

Name (Units)	Definition
$D$ (m)	Stem (root) diameter
$D'$ (m)	Xylem diameter
$\rho$ (m)	Thickness of the storage compartment
$V$ (m <sup>3</sup> )	Volume of the storage compartment
$l$ (m)	Length of the axis
$\varepsilon$ (MPa)	Elastic modulus of the storage compartment
$A$ (m <sup>2</sup> )	Area of the membrane separating the stem storage compartment from xylem
$P$ (MPa)	Turgor pressure in the storage compartment
$P_x$ (MPa)	Hydrostatic pressure in xylem
$\pi_s$ (MPa)	Osmotic pressure in the storage compartment
$\pi_x$ (MPa)	Osmotic pressure in the xylem
$Z$ (mol m <sup>-3</sup> s <sup>-1</sup> )	Maximum rate of solute accumulation in the storage compartment
$X$	Proportion of solutes that are not consumed through respiration catabolism and that remain soluble
$T$ (K)	Temperature

### Diameter Variation Components

The variation in diameter  $D$  is the result of elastic and thermal expansion and growth processes:

$$dD/dt = (dD/dt)_{el} + (dD/dt)_{th} + (dD/dt)_{gr} \quad (4)$$

Assuming that elastic expansion does not affect the xylem diameter  $D'$ , the first term in Equation 4 is defined by Equations 1 and 3 as:

$$(dD/dt)_{el} = 2(d\rho/dt)_{el} = 2(\rho/V)(dV/dt)_{el} \quad (5)$$

The relative elastic variation of the storage compartment volume is proportional to the variation of the turgor pressure  $P$  (MPa) in this compartment (Dale and Sutcliffe, 1986):

$$(dV/dt)_{el}/V = (dP/dt)/\varepsilon \quad (6)$$

where  $\varepsilon$  (MPa) is the elastic modulus. The elastic modulus increases with turgor and cell size (Tyree and Jarvis, 1982; Dale and Sutcliffe, 1986) and reaches an asymptote for high turgor and cell size. For the sake of simplification and to limit the number of parameters, a linear relationship was assumed. To take both relationships into account, the elastic modulus was assumed to be proportional to turgor and diameter:

$$\varepsilon = \varepsilon_0 PD \quad (7)$$

where  $\varepsilon_0$  (m<sup>-1</sup>) is a parameter.

Combining Equations 5, 6, and 7, the diameter variation resulting from elastic expansion was:

$$(dD/dt)_{el} = 2\rho(dP/dt)/(\varepsilon_0 PD) \quad (8)$$

In physics, the thermal expansion of the material (including wood) is described as being proportional to temperature ( $T$  in K). We considered that this law could be applied to a living plant and that the relative diameter variation resulting from temperature fluctuations was proportional to temperature change:

$$(dD/dt)_{th}/D = \alpha dT/dt \quad (9)$$

where  $\alpha$  is the coefficient of thermal expansion (K<sup>-1</sup>). The effect of growth may be represented as:

$$(dD/dt)_{gr} = (dD/d\rho)(d\rho/dt)_{gr} \quad (10)$$

Because  $D'$  can be considered to be constant compared with  $\rho$  for plastic growth on an hourly basis, the differentiation of  $V$  in Equation 3 is:

$$(d\rho/dt)_{gr} = \rho(dV/dt)_{gr}/V \quad (11)$$

When the turgor pressure  $P$  exceeds a threshold value  $Y$  (MPa), irreversible plastic growth occurs, as described by Lockhart's (1965) equation:

$$(dV/dt)_{gr}/V = \phi(P - Y) \quad \text{if } P > Y \quad (12)$$

$$(dV/dt)_{gr}/V = 0 \quad \text{if } P \leq Y$$

where  $\phi$  (MPa<sup>-1</sup> sec<sup>-1</sup>) is the extensibility of the cell walls.

Because the time frame of the model is longer than an hour, the growth of  $D'$  has to be considered to calculate  $dD/d\rho$  (Eq. 10). To take the growth of  $D'$  into consideration from a mechanistic point of view, it would be necessary to consider the process of differentiation of mature xylemic vessel, leading to a specific model which is not within our subject matter. That is why an empirical approach was used, based on the fact that the thickness of extensible tissues increases with the diameter of the organ, as shown for apple stems by Huguet (1985). An empirical relationship between  $\rho$  and  $D$  was used to calculate  $dD/d\rho$ :

$$\rho = a(1 - \exp[-bD]) \quad (13)$$

where  $a$  and  $b$  are parameters. Thus, it can be deduced that:

$$(dD/dt)_{gr} = (dD'/dt)_{gr} + 2(d\rho/dt)_{gr} = (d\rho/dt)_{gr}/$$

**Table II.** Model parameter values and significance

SD is given between parentheses for the estimated parameters. Values specific to stem or root or time period are indicated.

Name	Values	Definition
$\beta$	0.463 <sup>a</sup> (0.035)	Empirical parameter for initial conditions
$P_x(P(0) = 0)$	-2.9 MPa	Hydrostatic pressure of the xylem for which zero turgor was reached
$a$	2.968 <sup>b</sup> (0.166) $10^{-3}$ m	Allometric parameter
$b$	32 <sup>b</sup> (3) $m^{-1}$	Allometric parameter
$\alpha$	9.395 <sup>a</sup> (0.366) $10^{-5}$ K <sup>-1</sup>	Coefficient of thermal expansion
$L$	1.035 <sup>a</sup> (0.122) $10^{-4}$ m MPa <sup>-1</sup> s <sup>-1</sup>	Hydraulic conductivity of the membrane separating storage compartment from xylem
$\sigma$	1	Coefficient of reflection for solutes
$\gamma$	3.541 <sup>a</sup> (0.213) $10^{-5}$ MPa s <sup>-1</sup> K <sup>-1</sup> , July 31	Parameter of solute uptake by root
	3.640 <sup>a</sup> (0.162) $10^{-5}$ MPa s <sup>-1</sup> K <sup>-1</sup> , Aug. 19–21	Parameter of solute uptake by root
	3.330 <sup>a</sup> (0.196) $10^{-6}$ MPa s <sup>-1</sup> K <sup>-1</sup> , Sept. 2–16	Parameter of solute uptake by root
$\epsilon_0$	1.026 <sup>a</sup> (0.245) $10^3$ m <sup>-1</sup> , stem	Elastic modulus parameter
	0.363 <sup>a</sup> (0.021) $10^3$ m <sup>-1</sup> , root	Elastic modulus parameter
$\phi$	1.154 <sup>a</sup> (0.032) $10^{-3}$ MPa <sup>-1</sup> s <sup>-1</sup> , root	Extensibility of the cell walls
$Y$	0.9 MPa, root	Wall-yielding threshold pressure

<sup>a</sup> Parameter estimated through the model calibration using the Generalized Reduced Gradient method. <sup>b</sup> Parameter estimated independently through a nonlinear regression procedure.

$$[b(a - \rho)] \quad (14)$$

Combining Equations 11, 12, and 14, the diameter variation resulting from growth was obtained as a function of turgor pressure and  $\rho$ :

$$(dD/dt)_{gr} = \rho\phi(P - Y)/[b(a - \rho)] \quad (\text{if } P > Y) \quad (15)$$

$$(dD/dt)_{gr} = 0 \quad (\text{if } P \leq Y)$$

### Thickness of the Storage Compartment

For the sake of simplicity, it is assumed that the flow of water to the storage compartment is essentially a flow of xylem water. The change of volume  $(dV/dt)_f$  resulting from this flow is described by an equation derived from nonequilibrium thermodynamics (Katchalsky and Curran, 1965):

$$(dV/dt)_f = AL[P_x - P - \sigma(\pi_x - \pi_s)] \quad (16)$$

where  $L$  (m MPa<sup>-1</sup> s<sup>-1</sup>) is the radial hydraulic conductivity of the membrane separating the stem storage compartment from the xylem,  $A$  (m<sup>2</sup>) is the surface area of this membrane,  $P_x$  (MPa) is the hydrostatic pressure in the xylem,  $\pi_x$  (MPa) is the osmotic pressure in the xylem,  $\pi_s$  (MPa) is the osmotic pressure in the storage compartment, and  $\sigma$  is the reflection coefficient of the membrane to the solutes. Because  $\pi_x \ll \pi_s$ , it can be disregarded in Equation 16 and in the following calculations.

The total variation of the storage compartment thickness includes variations resulting from the horizontal flow of water and thermal expansion:

$$d\rho/dt = (d\rho/dt)_f + (d\rho/dt)_{th} \quad (17)$$

with  $(d\rho/dt)_f = (\rho/V)(dV/dt)_f$  and  $(d\rho/dt)_{th} = \rho\alpha dT/dt$  (from Eqs. 5, 9, and 11), which leads to:

$$d\rho/dt = L(P_x - P + \sigma\pi_s) + \rho\alpha dT/dt \quad (18)$$

combining Equations 16 and 17. The variation of  $\rho$  was dependent on turgor pressure and osmotic potential that had to be calculated.

### Turgor Pressure and Osmotic Potential

The variation of the turgor pressure results from the flow of water to the storage compartment. The balance between the solution inflow and elastic-plastic changes of the volume  $(dV/dt)_f = (dV/dt)_{el} + (dV/dt)_{gr}$  can be expressed using Equations 8, 12, and 16:

$$AL(P_x - P + \sigma\pi_s) = V[(dP/dt)/(\epsilon_0 PD) + \phi(P - Y)] \quad \text{if } P > Y \quad (19)$$

$$AL(P_x - P + \sigma\pi_s) = V[(dP/dt)/(\epsilon_0 PD)] \quad \text{if } P \leq Y$$

The turgor pressure variation can then be calculated:

$$dP/dt = \epsilon_0 L(P_x - P + \sigma\pi_s)PD/\rho - \epsilon_0 \phi PD(P - Y) \quad \text{if } P > Y \quad (20)$$

$$dP/dt = \epsilon_0 L(P_x - P + \sigma\pi_s)PD/\rho \quad \text{if } P \leq Y$$

According to the definition of Van't Hoff, the osmotic pressure is:

$$\pi_s = RTn_s/V \quad (21)$$

where  $R$  is the universal gas constant and  $n_s$  is the number of moles of solutes in volume ( $V$ ). Differentiation of Equation 21 over a period of time gives:

$$d\pi_s/dt = (RT/V)(dn_s/dt) - \pi_s(dV/dt)/V + \pi_s(dT/dt)/T \quad (22)$$



Considering a cell as a closed system where the amount of solutes,  $n_s$ , does not change with time and where the temperature is constant, only the second term in the right-hand side of Equation 22 is usually taken into account (Dainty, 1976). In higher plants, the uptake of solutes has to be accounted for, as described by the first term in the right-hand side. Daily and seasonal temperature variations lead to the last term of Equation 22. Assuming that solutes are transported to the growing stem by means of an active (and/or facilitated) mechanism, and using the Michaelis-Menten equation to describe the rate of the process, we have:  $dn_s/dt = ZXVC_p/(K_M + C_p)$ , where  $C_p$  is the solute concentration in the sap,  $Z$  is the maximum rate of the solute accumulation process considered to be constant, and  $X$  is the proportion of these solutes that are not consumed by respiration catabolism and remain soluble. If as a first approximation,  $K_M \ll C_p$ ,  $dn_s/dt \approx ZXV$ , and considering Equation 16 for volume variations, Equation 22 can be rewritten as:

$$d\pi_s/dt = \gamma T - \pi_s L(P_x - P + \sigma\pi_s)/\rho + \pi_s(dT/dt)/T \quad (23)$$

where  $\gamma = RXZ$  (MPa s<sup>-1</sup> K<sup>-1</sup>) is a parameter.

### Governing Equations

By combining Equations 4, 8, 9, 15, and 20, we obtain Equation 24:

$$dD/dt = 2L(P_x - P + \sigma\pi_s) + D\alpha(dT/dt) + \rho\phi(P - Y) \cdot \{1/[b(a - \rho)] - 2\} \quad (24)$$

Due to the restrictions in Equation 15, the last term in Equation 24 is equal to 0 if  $P \leq Y$ .

Equations 18, 20, 23, and 24 form a system of differential equations for  $P$ ,  $\pi_s$ ,  $\rho$ , and  $D$ , which can be solved numerically with given (inputted) functions of time  $P_x(t)$  and  $T(t)$ , and the initial values of respective variables.

### Initial Conditions and Parameterization

To run the model, initial values were needed for  $P$ ,  $\pi_s$ , and  $\rho$ . These values were approximated at the end of the night before the beginning of the simulation. At this time of the day, we can assume that the water potential of the storage compartment was equal to the xylem hydrostatic pressure ( $P_x$ ). In this case, the initial value of  $\pi_s$  can be calculated as:

$$\pi_s(0) = P(0) - P_x(0) \quad (25)$$

At this time of the day, the osmoregulation is probably low because the water potential is high and fairly stable. Under these conditions, the turgor pressure can be proportional to the hydrostatic pressure of the xylem as shown by Fanjul and Rosher (1984) on apple leaves:

$$P(0) = \beta[P_x(0) - P_x(P(0) = 0)] \quad (26)$$

where  $\beta$  is an empirical parameter estimated using the Generalized Reduced Gradient method in the calibration procedure and  $P_x(P(0) = 0)$  is the hydrostatic pressure of the xylem for which the zero turgor was reached. For  $P_x(P(0) = 0)$ , we used the value given by Fanjul and Rosher (1984) for apple leaves (-2.9 MPa) under well-watered conditions.

We measured the initial value of  $D$  and used it to compute initial  $\rho$  by means of Equation 13. By measuring the thickness of extensible tissues on three peach cultivars (see "Materials and Methods"), we could estimate the parameters of Equation 13 through a nonlinear regression procedure,  $a = 2.968 \cdot 10^{-3}$  m and  $b = 32$  m<sup>-1</sup>. The three cultivars followed the same general curve.

The wall-yielding threshold pressure,  $Y$ , has been observed in a variety of plant tissues (Green et al., 1971; Green and Cummins, 1974; Bradford and Hsiao, 1982) with values ranging from 0.1 to 0.9 MPa. Assuming that the threshold pressure had to be higher for stem or root tissues than for young tissues or individual cells on which most of the measurements had been done, we chose  $Y = 0.9$  MPa.

The virtual composite membrane is composed of several cell layers leading to possible cell-to-cell and apoplastic water flow. The reflection coefficient of the apoplast is usually close to 0, whereas along the cell-to-cell path, the presence of the membrane leads to a reflection coefficient close to 1 (Steudle, 2000). The overall tissue reflection will then be between 0 and 1. In our single cell model, most of the water has to cross the cell membrane, which is why we have adopted a high reflection coefficient ( $\sigma = 1$ ). Nevertheless, we evaluate its size through the sensitivity analysis.

The other parameters of the model ( $\alpha$ ,  $L$ ,  $\gamma$ ,  $\varepsilon_0$ , and  $\phi$ ) were estimated through the calibration procedure, using the Generalized Reduced Gradient method.

## RESULTS

### Calibration of Model

The parameter values and standard deviations are summarized in Table II. The coefficient of thermal expansion for peach stems was estimated on two stems, the diameter variations of which were measured before bud break. The evolution in time of diameter showed a decreasing trend of  $2.61 \cdot 10^{-8}$  and  $6.17 \cdot 10^{-8}$  m s<sup>-1</sup>, depending on the stem. Considering this decrease,  $\alpha$  (Eq. 9) was estimated to be equal to  $9.39 \cdot 10^{-5}$  K<sup>-1</sup>, which is close to the coefficients of thermal expansion for wood across the fibers ( $3\text{--}7 \cdot 10^{-5}$  K<sup>-1</sup>) given by Forsythe (1954) and Koshkin and Shirkevitch (1975). The overall percentage variation explained by the optimized curve fitting was 65%. Diameter variations due to temperature conditions and predicted by the model were lower than those

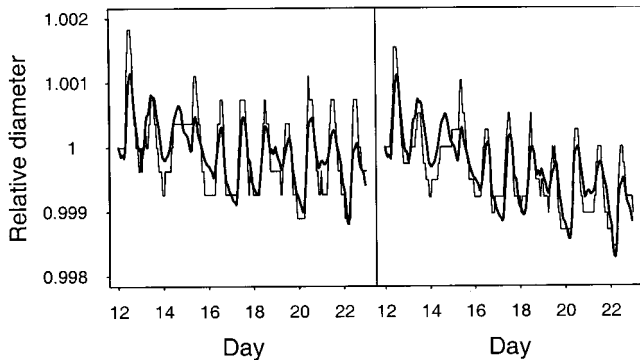


**Figure 2.** Diurnal variations of stem diameter with temperature in two peach stems in February before bud break. Relative diameter is calculated as the ratio "diameter:diameter at the beginning of the day." The thin lines represent the measurements and the thick lines represent the simulations.

measured (Fig. 2), probably because the temperatures recorded by the meteorological station had underestimated the maximal field temperatures. Measurement of surface stem temperature made with thermocouple at the same period of the year on other peach trees gave maximal temperatures 2.2°C to 4.8°C greater than the maximal temperature recorded by the meteorological station.

The Gotheron severe water stress treatment (GSS) was used to estimate  $\beta$  (Eq. 26), radial hydraulic conductivity  $L$  (Eq. 16), and elastic modulus parameter  $\varepsilon_0$  (Eq. 7) for the stem. The diameter variations of three stems were measured over a period of 24 h. The diameter growth of the stems was low and the diameter variation resulting from growth was not considered, which means that  $\gamma$  and  $\phi$  were set at 0. We estimated the empirical parameter  $\beta$  to be equal to 0.463. The parameter  $\varepsilon_0$  was estimated to be equal to  $1.026 \cdot 10^3 \text{ m}^{-1}$ , resulting in values for the elastic modulus  $\varepsilon$  ranging from 2 to 50 MPa. These estimates are within the range of the values obtained for giant algal cells (10–60 MPa) and higher plants tissues (0–30 MPa) as reported by Dainty (1976), Tyree and Jarvis (1982), and Dale and Sutcliffe (1986). Radial hydraulic conductivity ( $L$ ) was estimated to be equal to  $2.86 \cdot 10^{-8} \text{ m MPa}^{-1} \text{ s}^{-1}$ , which is in the range of the values obtained for giant algal cells ( $1.86 \cdot 10^{-8} - 2.78 \cdot 10^{-4} \text{ m MPa}^{-1} \text{ s}^{-1}$ ) and from cells of higher plant tissues ( $1.0 \cdot 10^{-10} - 1.67 \cdot 10^{-4} \text{ m MPa}^{-1} \text{ s}^{-1}$ ) as reported by Dainty (1976) and Dale and Sutcliffe (1986).

The overall percentage variation of stem diameter explained by the optimized curve fitting was 93% (Fig. 3).

The root data set collected from September 2 through 16 was used to estimate the growth parameters ( $\phi$  and  $\gamma$  in equations 14 and 23, respectively) because growth was well marked during this period. The parameters  $\alpha$ ,  $\beta$ , and  $L$  estimated for the stem were assumed to be acceptable for the root and  $\varepsilon_0$  only had to be reestimated. Tissue elasticity was

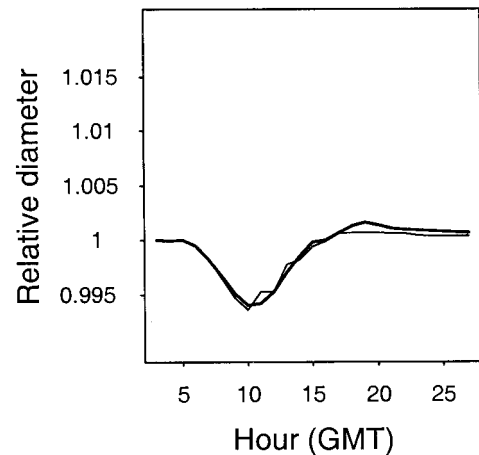


**Figure 3.** Mean diurnal variations of peach stem diameter on July 9 for the GSS treatment used for model calibration on stems. The mean was calculated on three stems. Relative diameter is calculated as the ratio "diameter:diameter at the beginning of the experiment." The thin lines are the measurements and the thick lines are the model simulations.

higher in the root ( $\varepsilon_0 = 0.363 \cdot 10^3 \text{ m}^{-1}$ ) than in the stem. The growth parameters were estimated to be  $\gamma = 9.25 \cdot 10^{-10} \text{ MPa s}^{-1} \text{ K}^{-1}$  and  $\phi = 3.19 \cdot 10^{-7} \text{ MPa}^{-1} \text{ s}^{-1}$ . The cell wall extensibility usually ranges from  $8.33 \cdot 10^{-6}$  to  $5.56 \cdot 10^{-5} \text{ MPa}^{-1} \text{ s}^{-1}$  (Hsiao et al., 1998), which is one order of magnitude higher than our estimate for the root tissues of plum. This is probably true because  $\phi$  is usually measured on young and very extensible tissues, whereas we were working on 5-year-old roots.

The overall percentage variation of root diameter explained by the optimized curve fitting was 97% (Fig. 4).

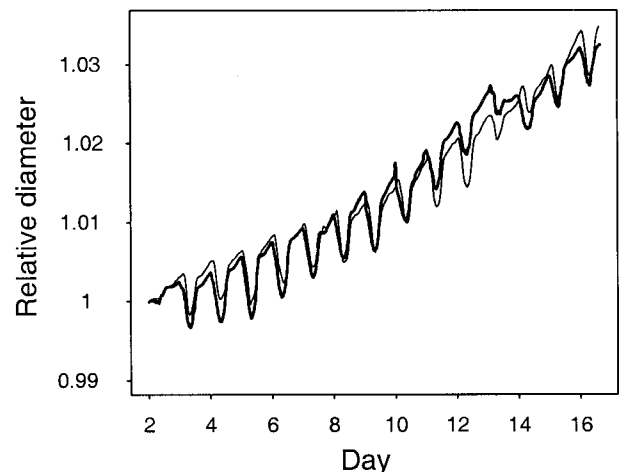


**Figure 4.** Variations of plum root diameter from September 2 through 16 used for model calibration on roots. Relative diameter is calculated as the ratio "diameter:diameter at the beginning of the experiment." The thin lines represent the measurements and the thick lines represent the model simulations.

### Model Test

To test the model, we used the data sets that had not been used for the calibration. The simulations of stem diameter variation in the Avignon and Gotheron experiments fit the observations quite well (Fig. 5). The model was able to reproduce the effect of water stress treatments on stem diameter variations at the two sites. For the root, the test was done on July 30 through 31 and August 19 through 21 data sets. Given the fact that growth rate was different between these two periods,  $\gamma$  had to be reestimated for each period ( $\gamma = 9.83 \cdot 10^{-9} \text{ MPa s}^{-1} \text{ K}^{-1}$  and  $1.01 \cdot 10^{-8} \text{ MPa s}^{-1} \text{ K}^{-1}$ , respectively). The model also made it possible to reproduce the diameter variation with time (Fig. 6) on an hourly and daily scale.

### Effect of Xylem Water Potential Variations on Storage Variables

As illustrated by the simulations performed on the plum root system for the period September 2 through 16, the daily variations of the xylem water potential resulted in lower daily variations of the turgor pressure and in much lower osmotic potential variations (Fig. 7). The coefficient of variation computed for the whole period was equal to 64%, 25%, and 5%, for the xylem water potential, the turgor pressure, and the osmotic potential, respectively. The elastic modulus was also sensitive to the water potential variations (Fig. 7) with a coefficient of variation (25.5%) very close to that of the turgor pressure to which it was highly correlated ( $R = 0.99$ ). The variation of osmotic potential, turgor pressure, and elastic modulus with the xylem water potential followed diurnal hysteresis loops (Fig. 8). Nevertheless, these variables

were highly correlated. The osmotic and water potentials were negatively correlated ( $R = -0.78$ ) when the turgor and the elastic modulus were positively correlated with the xylem water potential ( $R = 0.96$  and  $0.95$ , respectively). Although a marked hysteresis was observed, the water potential of the storage tissues was highly correlated to that of the xylem ( $R = 0.9$ ; Fig. 8).

### Sensitivity Analysis to Parameters

The sensitivity analysis was performed on the plum root system, using the environmental and water potential conditions of the period from September 2 through 16. The parameters of the model had a variation of  $\pm 20\%$  and the effect of this variation on the mean daily diameter growth rate and the mean shrinkage were assessed (Table III).

The model was very sensitive to the parameters  $\beta$  and  $P_x(P(0) = 0)$  used to estimate the initial value of  $P$ . A variation of these parameters induced an equivalent variation of the shrinkage and the growth rate variation was two or three times higher. This shows that a precise estimate of the initial  $P$  is needed to predict the actual daily growth rate and, to a lesser extent, the shrinkage. The shrinkage was not sensitive to the empirical parameters ( $a$  and  $b$ ) involved in the relationship between  $\rho$  and  $D$  (Equation 13), contrary to what was observed for radial growth rate.

Shrinkage and growth rate were not sensitive to the variations of the coefficient of thermal expansion ( $\alpha$ ). Nevertheless, some effect on shrinkage was observed when  $\alpha$  was decreased 10-fold.

The flow of water to the storage compartment depended on the hydraulic conductivity  $L$ , the variation

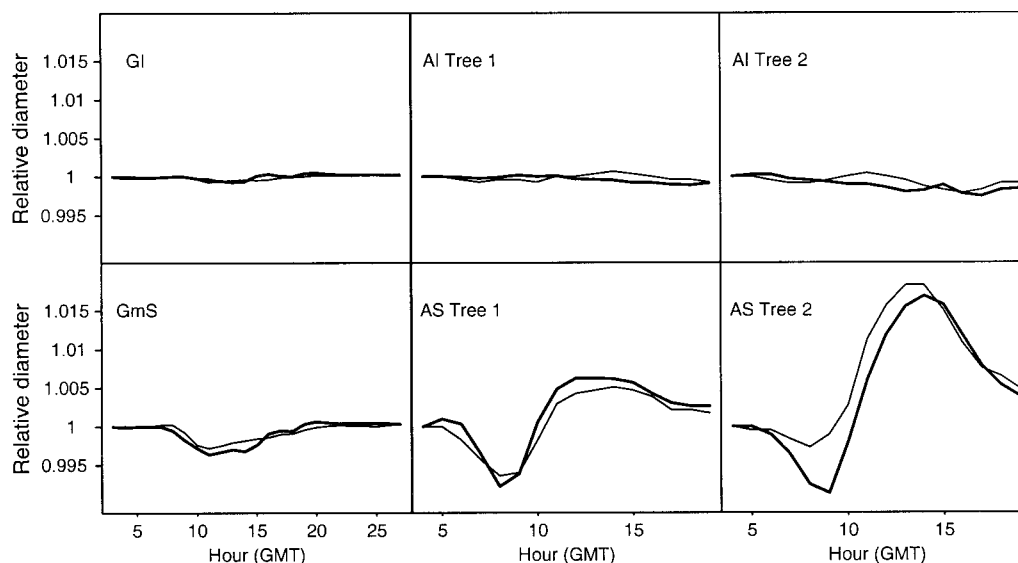


**Figure 5.** Diurnal variations of peach stem diameter for the treatments used for the model test (Gotheron well irrigated [GI], Gotheron mid-water stress [GmS], Avignon well irrigated [AI], and Avignon stressed [AS]). Relative diameter is calculated as the ratio "diameter:diameter at the beginning of the day." The thin lines represent the measurements and the thick lines represent the model simulations.

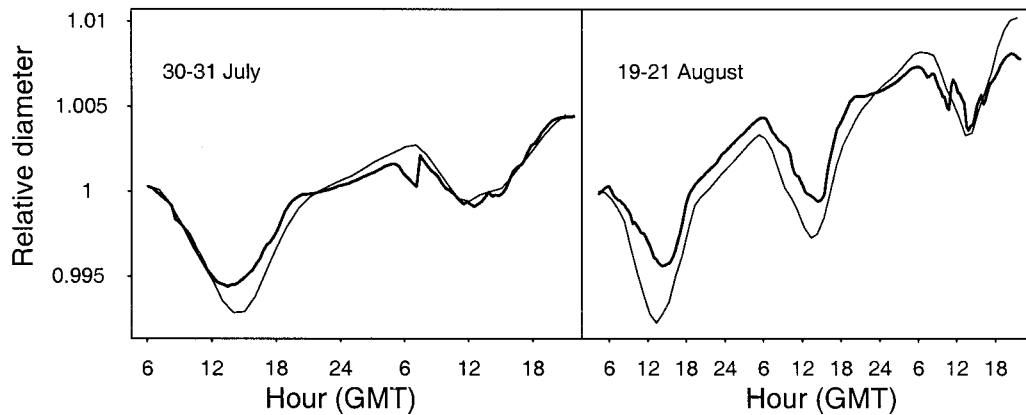


**Figure 6.** Diurnal variations of plum root diameter for the two periods used for the model test. Relative diameter is calculated as the ratio "diameter:diameter at the beginning of the experiment." The thin lines represent the measurements and the thick lines represent the model simulations.

of which (around  $2.86 \cdot 10^{-8} \text{ m MPa}^{-1} \text{ s}^{-1} \pm 20\%$ ) had no effect on diameter growth rate and shrinkage. For very low conductivity values (below  $1.39 \cdot 10^{-8} \text{ m MPa}^{-1} \text{ s}^{-1}$ ), daily growth rate and shrinkage decreased. It was more surprising that the daily growth rate also decreased for high conductivities (greater than  $2.78 \cdot 10^{-6} \text{ m MPa}^{-1} \text{ s}^{-1}$ ). According to the simulations, this can be explained by a turgor pressure which was often lower than the wall-yielding threshold pressure,  $Y$ . This low turgor pressure decreased the elastic modulus  $\varepsilon$ , and consequently increased shrinkage. Maximal growth was obtained for conductivity values ranging from  $1.67 \cdot 10^{-8}$  to  $2.78 \cdot 10^{-6} \text{ m MPa}^{-1} \text{ s}^{-1}$ , which included the conductivity values ( $L = 2.86 \pm 0.012 \cdot 10^{-8} \text{ m MPa}^{-1} \text{ s}^{-1}$ ) estimated for peach stem. The 20% decrease of the reflection coefficient ( $\sigma$ ) induced a 30% increase of shrinkage and a strong decrease of the growth rate (Table III). Shrinkage was not very sensitive to the variation of solute accumulation (parameter  $\gamma$ ). Growth was positively but slightly dependent on  $\gamma$  variations. The elastic modulus variation had no effect on growth and a proportional effect on shrinkage. The shrinkage was not sensitive to the plastic growth parameters. Growth and cell wall extensibility varied likewise when change of the threshold yield  $Y$  had a stronger effect.

#### Hysteresis between Xylem Water Potential and Diameter Variations

The relationship between stem diameter and xylem water potential simulated by the model was similar to that obtained from experimental data as illustrated by the Avignon AI and AS treatments (Fig. 9). Hysteresis was not marked on the well-irrigated treatment (AI) and no clear relationship between stem diameter and xylem water potential was observed. In case of water stress (AS), the general trend was an increase of stem diameter as xylem water potential increased. This general trend was disturbed by a strong hysteresis loop. For a given xylem water po-

tential, the stem diameter is lower during a period of increasing water potential (between 8 and 14 h Greenwich Mean Time) than during a period of decreasing water potential, which is in agreement with the results obtained on plants as different as cotton (Klepper et al., 1971) and peach tree (Garnier and

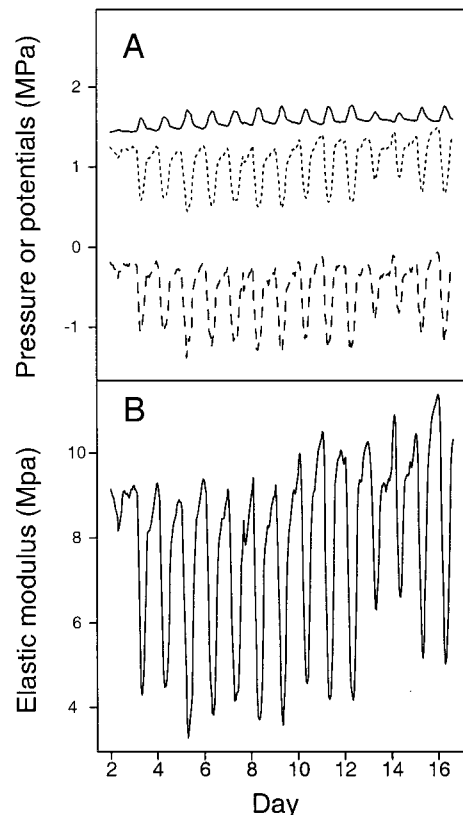


**Figure 7.** Variations of simulated turgor pressure (dotted line) and osmotic potential (unbroken line) of the storage compartment, and measured xylem water potential (broken line) from September 2 through 16 for plum root (A). The variations of the simulated elastic modulus are drawn in B.



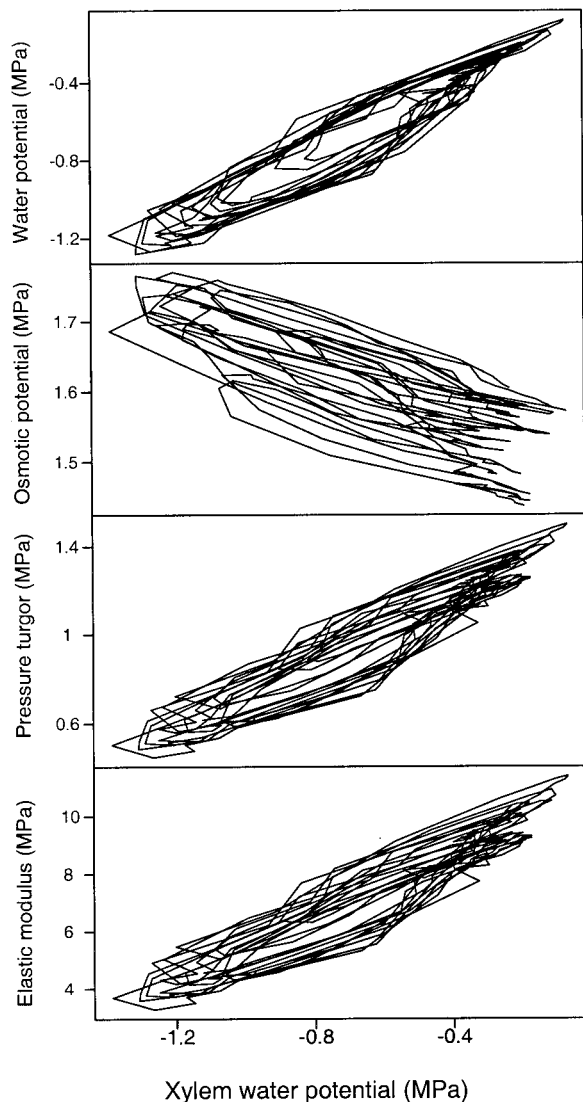


**Figure 8.** Relationships between simulated water potential, osmotic potential, pressure turgor, elastic modulus of the storage compartment, and measured xylem water potential. The simulations were performed from September 2 through 16 on plum root.

Berger, 1986). The hysteresis loop is caused by the delayed response of stem diameter compared with the xylem water potential. This delay results from the storage properties (growth, elasticity of tissues, and volume) and the radial hydraulic conductivity of the membrane separating the stem storage compartment from the xylem.

To analyze the effect of these properties on the degree of hysteresis, the diameter variation was simulated using the root parameters on September 3, which was a typical day for that season. Hysteresis was equally pronounced whether growth was considered ( $\phi = 0$  and  $\gamma = 0$ ) or not (Fig. 10). To analyze the effect of elasticity, volume of storage compartment, and conductivity, we multiply the values of  $\epsilon_0$ , radial hydraulic conductivity ( $L$ ) and initial thickness of the elastic tissues by 0.5 or 2. The effect was

significant with a higher hysteresis value as  $\epsilon_0$  and  $L$  decreased (Fig. 11). The initial thickness of elastic tissues resulted in higher variations of the hysteresis, which increased as thickness increased (Fig. 11).

## DISCUSSION

Earlier attempts have been made to better understand the relationship between water status and diameter variation. Molz and Klepper (1972) presented a theory explaining shrinking and swelling in the stem diameter of cotton plant, and Huck and Klepper (1977) proposed an empirical model based on this theory to estimate the water potential from stem diameter measurements. This theory is based on the passive diffusion flow of water, resulting from the radial propagation of the water potential in the phloem and cambial derivatives. It assumes a constant shrinkage modulus, which defines the water potential change required to induce a unit change in the volume (Molz and Klepper, 1972). As a matter of fact, the description of the different processes that take place are not based on a biophysical description. This is especially true for the water flow which is assumed to be diffusive in nature. So et al. (1979) developed a simpler dynamic method to convert stem diameter variation into leaf water

**Table III.** Effect of a  $\pm 20\%$  variation of the model parameters on the daily shrinkage and the diameter growth rate

Values are expressed as a percentage of the reference condition. The simulations used for the calculations were performed from Sept. 2 through 16 on the plum root.

Parameter and Level of Variation	Shrinkage	Diameter Growth Rate
Initial conditions		
$\beta + 20$	-20	+70
-20	+30	-65
$P_x(P[0] = 0) + 20$	+30	-67
-20	-20	+74
Allometric parameters		
$a + 20$	0	-19
-20	0	+33
$b + 20$	0	-19
-20	0	+23
Thermal coefficient		
$\alpha + 20$	0	0
-20	0	0
Water and solute flow parameters		
$L + 20$	0	0
-20	0	0
$\sigma - 20$	+30	-74
$\gamma + 20$	-4	+14
-20	+4	-8
Elastic variation parameter		
$\epsilon_0 + 20$	-17	0
-20	+17	0
Plastic growth parameters		
$\phi + 20$	0	+13
-20	0	-16
$Y + 20$	0	-46
-20	0	+49

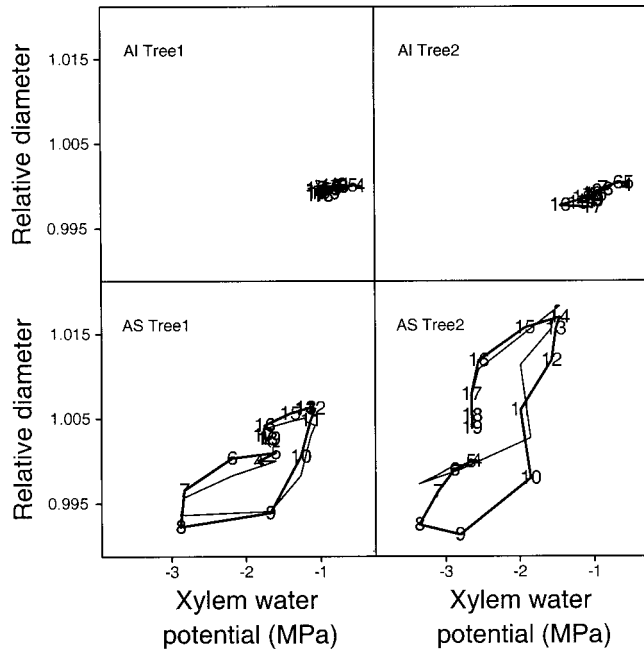


**Figure 9.** Relationship between the relative stem diameter and xylem water potential for the Avignon experiment (AI and AS). Relative diameter is calculated as the ratio “diameter:diameter at the beginning of the day.” The thin lines represent the measurements and the thick lines represent the model simulations. Figures on the lines represent the time (Greenwich Mean Time) of the day.

potential variation by introducing a shrinkage modulus and a plant response time as well to allow for the existence of hysteresis between water potential and stem diameter. Moreover, these attempts always neglected the plastic effect as well as the thermal dilatation of the tissues. The framework presented and developed here makes it possible to provide a better description of the relationship between water potential and stem variations using the principles of irreversible thermodynamics. It pieces together elements of existing theory and present knowledge of cell/tissue water relationships and uses them in a simulation model. Many studies deal particularly with water transfer at the cell or tissue scale (Steudle, 1994).

According to the model, the sensitivity of diameter variation to radial hydraulic conductivity was very low. For  $L$  ranging from  $1.7 \cdot 10^{-8}$  to  $2.8 \cdot 10^{-6} \text{ m MPa}^{-1} \text{ s}^{-1}$ , which is consistent with most hydraulic conductivity values found in scientific literature, the model predicted standard growth and shrinkage. The estimated hydraulic conductivity values were quite high ( $L = 2.86 \cdot 10^{-8} \text{ m MPa}^{-1} \text{ s}^{-1}$ ), which could explain the slight time lag observed by Simonneau et al. (1993), between the rate of change in the water compartment and the stem diameter in peach trees. The radial hydraulic conductivity is a very significant parameter of hysteresis between water potential and diameter, with a higher hysteresis for low values. Recent studies emphasize its variation as a function of the magnitude and the nature of the driving force, os-

motric or hydrostatic (Steudle, 1994), and the diurnal aquaporin expression (Clarkson et al., 2000). The radial hydraulic conductivity could then be considered as variable, but more information is needed to integrate this variation into the model. The reflection coefficient can be substantially lower than the unit as shown for roots (Steudle and Peterson, 1998). It can be explained by symplasmic connections between the cells of the storage compartment through plasmodesmata, and by transport of solutes with water through the apoplasm (Steudle, 1994). This reflection coefficient had a strong effect on shrinkage and growth. According to Equation 16, water influx decreases with simultaneous decreases of the reflection coefficient. As a consequence, growth and turgor pressure decreased, leading to a decrease of the elastic modulus and thus an increase of the shrinkage. The strong effect of the reflection coefficient implies that its possible variation has to be studied more thoroughly and included in models focusing on water flows, as shown by Steudle (1994) for modeling water transport across the roots.

Growth was neither very sensitive to small variations ( $\pm 20\%$ ) of the parameter  $\gamma$  involved in solute accumulation, nor to the extensibility of cell walls.

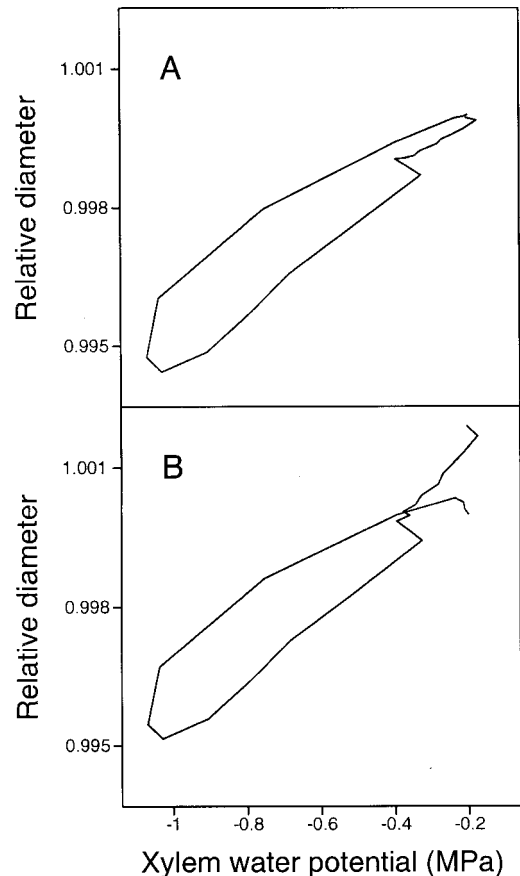


**Figure 10.** Simulated relationship between root diameter and xylem water potential for plum root on September 3, with (A) or without (B) growth.

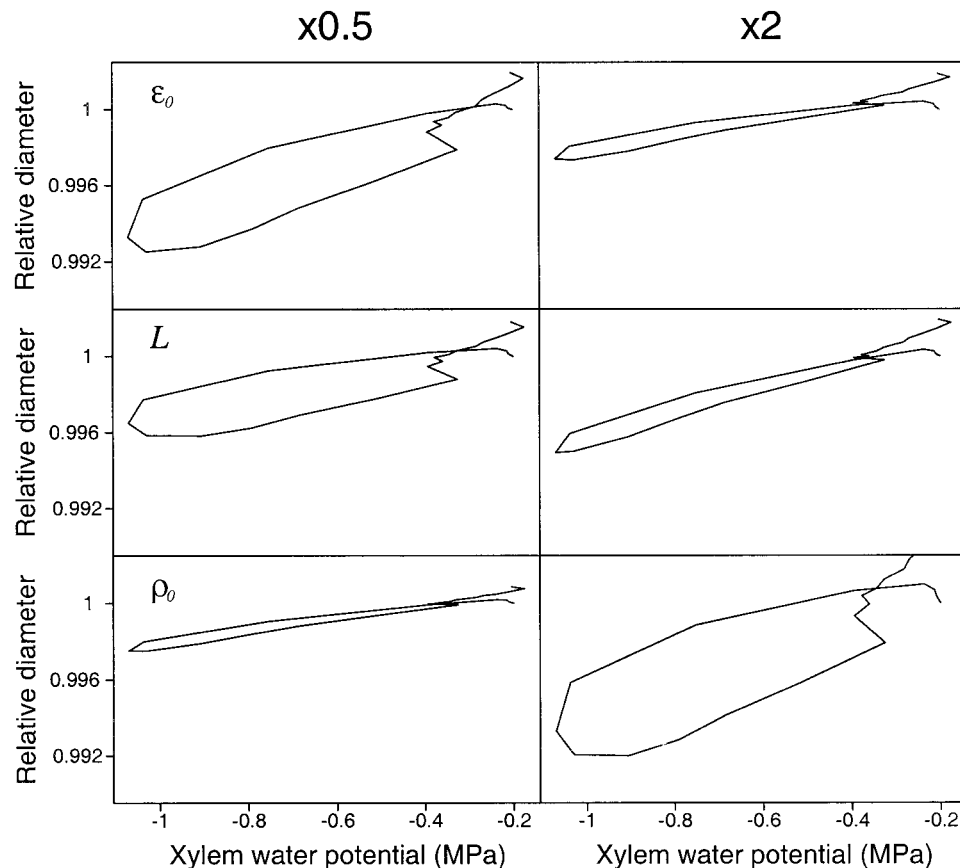


**Figure 11.** Sensitivity of hysteresis between root diameter and xylem water potential to elasticity parameter ( $\epsilon_0$ ), radial hydraulic conductivity ( $L$ ), and initial thickness of elastic tissues ( $\rho_0$ ) for plum root on September 3. Relative diameter is calculated as the ratio "diameter:diameter at the beginning of the day."  $\epsilon_0$ ,  $L$ , and  $\rho_0$  were multiplied by 0.5 or 2 as indicated at the top of the figure.

On the contrary, growth was highly sensitive to the threshold value  $Y$ . Further studies are needed to gain a better knowledge of  $Y$ . Growth is also sensitive to the allometric parameters  $a$  and  $b$ . The transition between elastic and plastic to rigid tissues with growth is accomplished via this empirical relationship between the thickness of the cork and the segment diameter (Equation 13). The simulated growth concerning the extensible tissue led to a simultaneous increase of the xylem. The aim of the study was to better understand the relationship between water potential and stem diameter variations rather than to describe the stem's growth under various plant water conditions over a long period of time. Therefore, a better description of the growth was not within our subject matter. The parameter  $\gamma$  is assumed to be independent of the temperature, which seems rather strange considering the growth. However, this parameter was estimated for each data set. Therefore, the calibration indirectly integrates the effect of temperature on this parameter. For the last period (mid-September), the parameter of solute uptake by the cell decreases 10-fold compared with the value obtained in the summer. Therefore, the limited time

scale of the model is only a consequence of the simplicity of the growth model.

Shrinkage intensity is affected by the parameter  $\epsilon_0$  because the elastic modulus is a significant component of the water storage capacity (Dainty, 1976). Moreover, the model postulates a linear relationship between  $\epsilon$  and the turgor pressure, rather than an asymptotic one. This simplification leads to a considerable overestimate of the elastic modulus with high turgor pressure. However, high turgor pressure is observed at night or in the morning. Therefore, the impact of this crude relationship could be limited in terms of stem diameter contraction.

Our model is very sensitive to the parameters  $\beta$  and  $P_x(P(0) = 0)$  used to calculate the initial value of the turgor pressure. Given that elastic modulus is proportional to turgor pressure and turgor pressure is the driving force for the growth, an increase of the initial turgor induces an increase of growth and a decrease of shrinkage. The initial condition (hydrostatic and osmotic pressure) was based on work done on apple leaves and through the calibration of  $\beta$ , an empirical parameter. It is then assumed that the root, the stem and the leaves have the same turgor loss

point. This seems pretty unlikely, but not many results are available in relation to pressure-volume parameters (Fanjul and Rosher, 1984).

Several parameters that were estimated indirectly via the calibration procedure or taken from other studies ( $L$ ,  $\sigma$ ,  $\varepsilon_0$ ,  $\phi$ , and  $\gamma$ ) could be measured directly. The hydraulic water conductivity and the solute selectivity of the membranes could be directly assessed using an approach similar to that of Steudle and coworkers (Steudle, 1994). A pressure probe could be mounted on the stem segment and pressure relaxation experiments could be done to estimate such parameters. The elastic modulus parameter could also be assessed using the pressure-volume relationship on a sample of non-xylem material. To estimate the initial turgor more accurately than with Equation 26, a measurement of tissue turgor could be made. For that purpose, a sample of the extensible tissue could be collected and placed in a psychrometer, which would make it possible to measure the total water potential. Next, the tissue could be plunged into liquid nitrogen, which would make it possible to measure the osmotic potential.

Despite the simplicity of the model, the simulations showed that the model accounts for differences in diameter variation according to temperature, solute accumulation (parameter  $\gamma$ ), and xylem water potential. It is a useful tool for the comprehensive study of the effect of variations of the xylem water potential on the diurnal and weekly diameter variation. It predicts that a given variation of water potential induces a lower variation of turgor pressure and only a slight change of the osmotic potential. These predictions are very close to observations made by McFadyen et al. (1996) of variations of turgor pressure and osmotic potential in peach flesh according to different levels of leaf water potential. The model also predicts strong positive correlation between the xylem water potential, the turgor pressure, and the elastic modulus, in agreement with the experimental results of Fanjul and Rosher (1984) on apple leaves, and Urban et al. (1994) on the stem of rose plants. On the other hand, the osmotic potential was found to be negatively correlated to the water potential in the case of apple leaves (Fanjul and Rosher, 1984).

The "single cell" approach is a very useful simplification, making it possible to take the different processes leading to stem diameter variation into account on a semimechanistic level. These different processes are the thermal dilatation of the material, the elasticity of the cell in response to change in volume, and the irreversible plastic growth. The single cell approach led to several assumptions. The stem (root) organ is decomposed on an elastic and a nonelastic cylinder. The nonelastic inner cylinder is made up of a single, homogeneous material (in other words, the mature xylem). On the other hand, the outer cylinder is made up of various components (bark, phloem, cortex, cambia, and immature xylem).

This cylinder includes a plastic growth zone (cambia) and an elastic zone (mature tissue). Therefore, we are not assuming that the tissue is homogeneous but rather that it is a composite, lumping together different types of tissue. In this case, the estimated parameters correspond with parameters associated with these different associated tissues and have no real meaning.

An alternative would be to take a two-cell approach and divide the model into a plastic growth zone (vascular and cork cambia) and an elastic zone (mature tissue). This approach could lead to a better description, as these parameters are known to vary from immature to mature tissue. Moreover, the cambia is an area where cell division (Esau, 1977) and expansion occur, whereas the mature tissue presents only elastic change to variations in turgor pressure. This knowledge could then be incorporated into a growth model based on the cellular level, introducing the cell division and cell expansion processes, but able to describe the tissue level growth as a function of water status (Arkebauer and Norman, 1995). Moreover, a better description of the system could be given by introducing the apoplasm. However, little is known about its role and more in-depth studies will have to be made, not only concerning the apoplastic barriers for water transfer but also in relation to its water content variations and its possible role in water storage. This type of detailed compartmentalization is difficult to assess because of the lack of experimental data.

The model was applied to peach stem and plum root but there is no restriction concerning its application to other species. It also gives an effective basis for integrating water storage compartments and diameter growth into water transfer models within the plant architecture, as was recently proposed by Doussan et al. (1998a, 1998b).

## MATERIALS AND METHODS

### Plant Material

In 1997, we studied a 3-year-old plum (*Prunus domestica* × *Prunus spinosa*, Damas GF1869) root from a tree planted in an orchard of the INRA Avignon Center. The tree was 2.5 m high and the root system had colonized nearly a one-half sphere with a radius of 3 m.

All the peach trees (*Prunus persica* L. Batsch cv "Big Top" on *Sylvestris* sp. rootstock) studied were potted in 80-L containers containing one-third turf and two-thirds volcanic substrate outdoors at the INRA Avignon Center (southeastern France) and the INRA Gotheron station (120 km north of Avignon), in March 1993. They were 1.5 to 2.0 m high and 1.0 to 1.5 m wide for the 1997 through 1998 period of study. Their fruit load was 100 to 400 fruits per tree.

All the trees were goblet trained and received routine horticultural care except for irrigation, which varied according to the treatments.



Subsets of the plant material were used to study: (a) the thermal expansion alone, (b) the thermal expansion and the water storage in extensible tissues, and (c) the thermal expansion, the water storage in extensible tissues, and the radial growth.

In the subset used to study the thermal expansion alone, two peach trees were studied in Avignon during the winter of 1997. This period of measurement was chosen to estimate thermal expansion parameters on peach stem because diurnal temperature variation was high (almost 17°C at the INRA meteorological station), diameter variation due to tree transpiration was low, and growth was not taking place.

Two experiments were carried out in 1998 to calibrate and test the model (see b above) on peach stems. They were performed to obtain very different stem diameter variations in response to water supply. In Avignon, two trees underwent trickle irrigation during the whole growing season (AI) and two trees received only 20% of the water given to the AI treatment from June 12 through the beginning of July (AS). At Gotheron, three groups of three trees were submitted to different types of irrigation treatments. One group was irrigated according to the AI treatment in Avignon (GI), one group received 40% of the water given for the GI treatment from mid-June through the end of July (Gotheron moderate water stress [GmS]), and the last group received only 15% during the same period (GSS).

To optimize the model calibration and definition of the parameters concerning variation of water flow and elasticity of extensible tissues, we used the GSS treatment, for which the shrinkage was high and the radial growth was stopped. During the measurement period, the radial growth was also stopped in the other treatments because of the high fruit load. These treatments were used to test the model on peach stems with no growth.

The application of the model (see c above) to growing organs was performed for roots. A growing plum root was studied in 1997. The studied plum tree received a routine irrigation. Three sets of data were obtained at three different periods during the summer. The most important data set was used to calibrate the model and estimate growth parameters, and the other sets were used to test it.

## Measurements

An estimate of the thickness of extensible tissues considered as non-mature xylem tissues (growing part of xylem, phloem, cambia, and inner bark) is needed. A sample of 20 stems was harvested on peach cv "Big Top" trees in 1997 and 1998 for this purpose. Two additional samples from "Opale" ( $n = 15$  stems) and "Suncrest" ( $n = 16$  stems) peach cultivars were collected from the INRA Avignon orchard in 1996. Stem diameter of these samples ranged from 5 to 100 mm. The thickness of extensible tissues was also measured on the studied plum root.

Stem diameter variations were continuously measured on the two peach cv "Big Top" trees used to study the thermal expansion. Stems with diameters of 27 and 39 mm were measured from February 12 through 22 in Avignon.

The xylem water potential and the stem diameter variations were measured every hour from 4 AM to 7 PM solar time on June 24 for AI and AS, and from 3 AM on July 9 to 3 AM on July 10 for GI, GmS, and GSS. The stem diameter and water potential were measured on each tree, except at Gotheron where the water potential was measured on one tree per treatment at a given time. The stem diameters ranged from 18.6 to 57.5 mm.

Similar measurements were performed for the plum root with an 18.5- to 21-mm diameter during three different periods: July 30 through 31, August 19 through 21, and September 2 through 16.

Stem and root diameter variations were measured using linear variable differential transformers (LVDTs) mounted on an INVAR frame (Li et al., 1989). The INVAR (Goodfellow, France) was chosen because this alloy has a very low coefficient of thermal expansion. The sensors were connected to a specific "Pepista" microcomputer to record the data (Pelloux et al., 1990). The xylem water potential of the stem was measured with a pressure chamber. The day before the measurements, leaf samples were selected and each leaf was individually enclosed in a plastic bag and wrapped in aluminum foil for the night. This inhibits leaf transpiration and makes it possible for the water potential in the leaf xylem to be in equilibrium with that of stem xylem at the point of attachment of the petiole (Simonneau and Habib, 1991). Measurements were performed on two to three leaves every hour on each tree. The water potential used in the simulations is the mean value per hour and per tree in Avignon and the mean value per hour and per treatment in Gotheron. The xylem water potential of the root was measured with a psychrometer located close to the LVDT. A section of sapwood was denuded by removing the bark, the phloem and the cambium layers. The sapwood area was thoroughly rinsed with distilled water and wiped off (Dixon, 1984). The thermocouple chamber was sealed over the root xylem vessels. A temperature-corrected stem psychrometer made it possible to correct the water potential resulting from the temperature gradient between the measurement junction and the sample (Vanderschmitt and Daudet, 1994). The psychrometer was connected to a datalogger (Campbell CR7, Untd. Sc.) to enable continuous measurement of both the water potential and the tissue temperature.

Such temperature measurements were not available for the peach stem. That is why we used the temperature recorded by the INRA meteorological stations located close to the experiment fields.

## Modeling Technique

Simulation of both diurnal and weekly processes were based on an hourly scale. It was also used as the time frame in the numerical integration. The computer program was written using Advanced Continuous Simulation Language (MGA Software, 1995). The differential equations were solved numerically by the first order Runge-Kutta method. Advanced Continuous Simulation Language Optimize (MGA Software, 1996) was used for the model calibration

to estimate parameters which could not be determined in independent experiments. Parameters were estimated by maximizing likelihood using the Generalized Reduced Gradient method. Using the log of the likelihood function, the probability of obtaining our set of measured diameter values was calculated, assuming that the model with its current set of adjustable parameter values was correct. Using the Generalized Reduced Gradient optimization algorithm, the values of adjustable parameters were systematically changed until we obtained the set of values that maximized the log likelihood function. The resulting values yielded the highest calculated probability of obtaining the data that we did. We could then infer that that set of values was the most likely to be correct.

## ACKNOWLEDGMENTS

We gratefully acknowledge T. Girard and R. Laurent for their assistance during the field experiments. We thank F. Lescourret for helpful comments on this paper and G. Rigou (INRA Translation Unit, Unité Centrale de Documentation, Jouy-en-Josas) and G. Wagman for revising the manuscript.

Received June 14, 2000; returned for revision October 13, 2000; accepted December 28, 2000.

## LITERATURE CITED

- Arkebauer TJ, Norman JM, Sullivan CY (1995) From cell growth to leaf growth: III. Kinetics of leaf expansion. *Agron J* **87**: 112–121
- Bradford KJ, Hsiao TC (1982) Physiological responses to moderate water stress. In OL Lange, PS Nobel, CB Osmond, H Ziegler, eds, *Physiological Plant Ecology II: Water Relations and Carbon Assimilation*. Springer-Verlag, Berlin, pp 263–324
- Brough DW, Jones HG, Grace J (1986) Diurnal changes in water content of the stems of apple trees, as influenced by irrigation. *Plant Cell Environ* **9**: 1–7
- Clarkson et al. (2000) Root hydraulic conductance: diurnal aquaporin expression and the effects of nutrient stress. *J Exp Bot* **342**: 61–70
- Dainty J (1976) Water relations of plant cells. In U Lüttge, MG Pitman, eds, *Encyclopedia of Plant Physiology*, New Series, Vol 2A. Springer-Verlag, Berlin, New York, pp 12–35
- Dale JE, Sutcliffe JF (1986) Water relations of plant cells. In FC Steward, ed, *Plant Physiology, Water and Solutes in Plants*, Vol. 9. Academic Press, Orlando, FL pp 1–48
- Dixon MA, Tyree MT (1984) A new stem hygrometer, corrected for temperature gradients and calibrated against the pressure bomb. *Plant Cell Environ* **7**: 693–697
- Doussan C, Pagès L, Vercambre G (1998a) Modeling of the hydraulic architecture of root systems: an integrated approach to water absorption model description. *Ann Bot* **81**: 213–223
- Doussan C, Vercambre G, Pagès L (1998b) Modeling of the hydraulic architecture of root systems: an integrated approach to water absorption distribution of axial and radial conductances in maize. *Ann Bot* **81**: 225–232
- Esau K (1977) *Anatomy of Seed Plants*, Ed 2. J. Wiley, New York, p 550
- Fanjul L, Rosher PH (1984) Effects of water stress on internal water relations of apple leaves. *Physiol Plant* **62**: 321–328
- Fishman S, Génard M (1998) Model of fruit growth based on biophysical description of main contributing processes: simulation of seasonal and diurnal dynamics of weight. *Plant Cell Environ* **21**: 739–752
- Forsythe WE (1954) *Smithsonian Physical Tables*. Smithsonian Institution, Washington, DC
- Garnier E, Berger A (1986) Effect of water stress on stem diameter changes of peach growing in the field. *J Appl Ecol* **23**: 193–209
- Green PB, Cummins WR (1974) Growth rate and turgor pressure: auxin effect studied with an automated apparatus for single coleoptiles. *Plant Physiol* **54**: 863–869
- Green PB, Erickson RO, Buggy J (1971) Metabolic and physical control of cell elongation rate: in vivo studies in *Nitella*. *Plant Physiol* **47**: 423–430
- Hsiao TC, Frensch J, Rojas-Lara BA (1998) The pressure-jump technique shows maize leaf growth to be enhanced by increases in turgor only when water status is not too high. *Plant Cell Environ* **21**: 33–42
- Huck MG, Klepper B (1977) Water relation of cotton: II. Continuous estimates of plant water potential from stem diameter measurements. *Agron J* **69**: 593–597
- Huguet JG (1985) Appréciation de l'état hydrique d'une plante à partir des variations micrométriques de la dimension des fruits ou des tiges au cours de la journée. *Agronomie* **5**: 733–741
- Katchalsky A, Curran PF (1965) *Nonequilibrium Thermodynamics in Biophysics*. Harvard University Press, Cambridge, MA
- Klepper B, Browning VD, Taylor HM (1971) Stem diameter in relation to plant water status. *Plant Physiol* **48**: 683–685
- Koshkin NI, Schirkevitch MI (1975) *Handbook of Elementary Physics*. Nauka, Moscow
- Kozlowski TT (1972) Shrinking and swelling of plant tissues. In Kozlowski TT, ed, *Water Deficits and Plant Growth*, Vol 3. Academic Press, New York, pp 1–64
- Li SH, Huguet JG, Bussi C (1989) Irrigation scheduling in a mature peach orchard using tensiometer and dendrometers. *Irrigation Drainage Syst* **3**: 1–12
- Lockhart JA (1965) An analysis of irreversible plant cell elongation. *J Theor Biol* **8**: 264–275
- Mcfadyen LM, Hutton RJ, Barlow EWR (1996) Effects of crop load on fruit water relations and fruit growth in peach. *J Hortic Sci* **71**: 469–480
- MGA Software (1995) *Advanced Continuous Simulation Language (ACSL) Reference Manual*. MGA Software, Concord, MA
- MGA Software (1996) *ACSL Optimize: User's Guide*. MGA Software, Concord, MA
- Molz FJ, Ikenberry E (1974) Water transport through plant cells and cell walls: theoretical development. *Soil Sci Soc Am Proc* **38**: 699–704

- Molz FJ, Klepper B** (1972) Radial propagation of water potential in stems. *Agron J* **64**: 469–473
- Molz FJ, Klepper B** (1973) On the mechanism of water-stress-induced stem deformation. *Agron J* **65**: 304–306
- Parlange JY, Turner NC, Waggoner PE** (1975) Water uptake, diameter change, and nonlinear diffusion in tree stems. *Plant Physiol* **55**: 247–250
- Pelloux G, Lorendeau JY, Huguet JG** (1990) Pepista: translation of plant behavior by the measurement of diameters of stem or fruit as a self-adjusted method for irrigation scheduling. In R Kuhlmann, ed, *Third International Congress for Computer Technology*. Deutsche Landwirtschafts-Gesellschaft, Frankfurt-sur-le-Main, Germany, pp 229–235
- Simmoneau T, Habib R** (1991) The use of tree root suckers to estimate the root water potential. *Plant Cell Environ* **14**: 585–591
- Simmoneau T, Habib R, Goutouly JP, Huguet JG** (1993) Diurnal changes in stem diameter depend upon variations in water content: direct evidence in peach trees. *J Exp Bot* **44**: 615–621
- So HB, Reicosky DC, Taylor HM** (1979) Utility of stem diameter changes as predictors of plant canopy water potential. *Agron J* **71**: 707–713
- Steudle E** (1994) Water transport across roots. *Plant Soil* **167**: 79–90
- Steudle E** (2000) Water uptake by roots: effects of water deficit. *J Exp Bot* **51**: 1531–1542
- Steudle E, Murrmann M, Peterson CA** (1993) Transport of water and solutes across maize roots modified by puncturing the endodermis: further evidence for the composite transport model of root. *Plant Physiol* **103**: 335–349
- Steudle E, Peterson CA** (1998) How does water get through roots? *J Exp Bot* **49**: 775–788
- Tyree MT, Jarvis PG** (1982) Water in tissues and cells. In OL Lange, PS Nobel, CB Osmond, H Ziegler, eds, *Physiological Plant Ecology II: Water Relations and Carbon Assimilation*. Springer-Verlag, Berlin, pp 35–77
- Urban L, Fabret C, Barthélémy L** (1994) Interpreting changes in stem diameter in rose plants. *Physiol Plant* **92**: 668–674
- Vanderchmitt E, Daudet FA** (1994) The origin and theoretical correction of thermal gradients in thermocouple psychrometers. *Plant Cell Environ* **17**: 97–104
- Zhu GL, Boyer JS** (1992) Enlargement in Chara studied with a turgor clamp. *Plant Physiol* **100**: 2071–2080
- Zimmerman MH, Milburn JA** (1982) Transport and storage of water. In OL Lange, PS Nobel, CB Osmond, H Ziegler, eds, *Physiological Plant Ecology II: Water Relations and Carbon Assimilation*. Springer-Verlag, Berlin, pp 135–151